Chemical Papers (2023) 77:1201–1211
https://doi.org/10.1007/s11696-022-02535-z

ORIGINAL PAPER

Porous Co_3O_4 nanospheres synthesized via solution combustion method for supercapacitors

Anjum Afrooze[1] · Dadamiah P. M. D. Shaik[2]

Received: 21 July 2022 / Accepted: 3 October 2022 / Published online: 26 October 2022

Abstract

Solution combustion method is a low-cost, simple, fast and productive technique for the synthesis of nanosized particles, and therefore, it has been used for the production of a variety of fine complex oxide powders for several advanced applications, including catalysts, fuel cells and energy storage. In this study, porous cobalt oxide nanospheres have been successfully synthesized by combustion method using cobalt nitrate hexahydrate ($Co(NO_3)_2.6H_2O$) and urea (NH_2CONH_2) as precursors at low temperature. The microstructural, dielectric, magnetic and electrochemical properties of the prepared cobalt oxide nanospheres are studied. The XRD spectra exhibited (220), (311), (222), (400), (422), (511), (440) orientations which corresponds to cubic structure of Co_3O_4 with $Fd\bar{3}m$ (227) space group. The crystallite size is estimated using Scherrer's formula and is found to be 8 nm. The SEM analysis reveals the appearance of spherical grains with an average grain size of 30 nm and variable pores of 7 nm in size. The presence of cobalt–oxygen bonding and the microstructure of the synthesized sample are confirmed from the Raman and FTIR studies. The dielectric studies show that the dielectric constant and dielectric loss of the sample decrease with frequency. The magnetic modules show the ferromagnetic nature of Co_3O_4 nanospheres. The supercapacitive behavior of Co_3O_4 nanospheres in 1 M KOH aqueous electrolyte shows a high specific capacitance of 182 Fg^{-1} at a current density of 0.5 Ag^{-1} and good electrochemical stability even after 2000 cycles.

Keywords Porous Co_3O_4 nanospheres · Solution combustion method · Specific capacitance · Aqueous electrolytes

Introduction

Energy conversion and storage technique has to be greatly explored in the field of research in order to meet the demands of energy in the present world and next generation. In the present world, the most important energy storage devices are batteries, capacitors and electrochemical capacitors (ECs). Among all these energy storage devices, the electrochemical capacitors are using to fill the power and energy gap between batteries and conventional capacitor owing to its long life span, high power density and good charging/discharging characteristics. As one of the key electrochemical energy storage devices, electrochemical capacitors also known as supercapacitors have, especially, shown great potential in recent years to meet the short-term power needs and energy demands over the timescale of 0.1–100 s (P. J. Hall et al. 2010). Their excellent power handling characteristics when combined with various primary energy sources allow engineers to utilize them as an attractive power solution for an increasing number of applications in order to match the specification of the primary energy sources closer to that of the average power demand in each particular case. However, to fully exploit the potential of ECs in the field of energy storage, advanced materials/electrolytes are required (M. Mirzaeian et al. 2017). One of the advances is exploring the nature of electrode material with their suitable electrolyte. The nature of electrode material governs the storing and releasing the energy of supercapacitors by accumulating charges at the interface of electrolyte and electrode or by speedy reversible oxidation–reduction reaction or by both. Nanosized metal oxide particles with porous nature are extensively used in electrochemical chemical capacitors due to high specific surface area-to-volume ratio. Transition metal oxides like MnO_2, IrO_2, RuO_2, V_2O_5, NiO, Mn_3O_4 and TiO_2 are a group of very promising supercapacitor electrode

✉ Dadamiah P. M. D. Shaik
rahilsp@gmail.com

[1] Department of Chemistry, Career Point University, Kota, Rajasthan, India

[2] Career Point University, Kota, Rajasthan, India

materials. Among transition metal oxides, ruthenium oxides with multiple redox states and good electrical conductivity are commonly used as a pseudocapacitor electrode (DPMD Shaik et al. 2018). However, due to expensive and toxic nature of RuO_2 (Wang et al. 2014), use of RuO_2 is limited; hence, alternate electrode materials for supercapacitors have to be explored. Henceforth, developing the electroactive materials with high reversible oxidation–reduction reactions and high specific surface area is an investigative area of electrochemists. Moreover, these materials must be economical. Researchers suggest the low energy density and high self-discharge of supercapacitors can be resolved by improving the capacitance of the supercapacitors and which can be further improved with the selection of suitable electrode material (Naresh et al. 2019). Works like synthesis of three-dimensional porous nanostructures with high specific surface area essential to enhance the capacitance of supercapacitors demonstrated better electrochemical performance due to its delightful structural morphology (Naresh et al. 2021).

Research shows that the spinel porous nanostructured Co_3O_4 is found to be one of the potential electrode materials because of its being economical, less toxic nature and possessing intrinsically high capacity (Zhang et al. 2013). Among the library of various transition metal oxides, cobalt oxide (Co_3O_4) emerged as a shining star on the horizon of metal oxides. It has high surface-to-volume ratio, simple preparation method, outstanding chemical durability, promising ratio of surface atoms and diverse morphology, which makes it more prominent in the family of transition metal oxides (Numan et al. 2016). Added to this, Co_3O_4 has greater stability and it finds many applications in various areas (Naresh et al. 2019; DPMD Shaik et al. 2021; Yildirim and Kilis 2019; Salunkhe et al. 2015). It is worthy to be noted that earlier work has been done with cobalt oxide nanoparticles as tubular structures with the integration of Co_3O_4 hollow nanoparticle by Zhang et al. (2017). Cobalt oxide materials can be considered as superior materials for supercapacitor application, due to fact that they have high theoretical capacitance values (~ 3,600 Fg^{-1}), low cost, environmental friendliness, high electrochemical stability, etc.(Salunkhe et al. 2015; Liu et al. 2016; Farhadi et al. 2013). The other points which reflect that Co_3O_4 electrode is efficient are its resistivity to corrosion and retention of performance for long time. There are fewer reports available on the electrochemical properties of Co_3O_4 nanospheres in different electrolytes along with dielectric and magnetic properties. Therefore, in the present investigation, solution combustion method (Gu et al. 2007; Wen et al. 2012) has been used to synthesize porous Co_3O_4 with nanodimensions at low temperatures and a detailed study has been executed to explore the electrochemical properties of prepared porous Co_3O_4 nanospheres in different aqueous electrolytes for their effective use in supercapacitors along with their dielectric and magnetic properties.

Experimental procedure

In the typical preparation, the porous Co_3O_4 nanospheres are synthesized by solution combustion technique. The procedure starts with the collection of two precursors, cobalt nitrate hexahydrate ($Co(NO_3)_2.6H_2O$) and urea (NH_2CONH_2) in equimolar ratio in 100 ml of deionized water and kept under continuous stirring for half an hour. Then, the solution is kept in a pre-heated muffle furnace at 150 °C for 1 h. During the synthesis, exothermic reactions are taking place with release of gases. Then, the furnace is turned off and left for 8 h to bring it to room temperature. Finally, the Co_3O_4 black powder is collected and the microstructural, morphological, dielectric, magnetic and electrochemical properties are studied systematically by means of techniques compiled in Table 1.

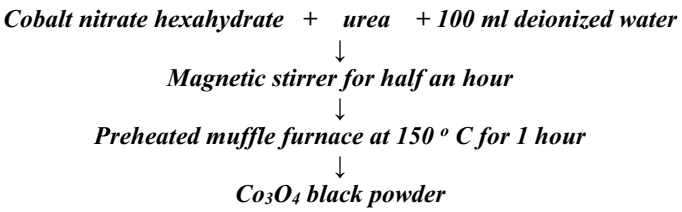

Flow Chart of porous Co_3O_4 nanospheres synthesis

Table 1 The information of structural properties and chemical analysis of as-prepared porous Co_3O_4 nanospheres

S. No.	Properties studied	Type of characterization	Instrument
1	Structural	XRD	CuK_α ($\lambda = 0.154$ nm) radiation source filtered by Ni thin film at a scan speed of 0.05° per second in the 2θ range 20–80°
2	Structural and vibrational	Raman spectra and FTIR	Raman Spectroscopy using Horiba Jobin Yvon Lab RAM HR800UV Raman spectrometer Bruker instrument
3	Morphology	Scanning electron microscopy (SEM)	Carl ZEISS (Model EVO MA15) morphology and chemical composition of the sample in high vacuum
4	Chemical composition	Energy-dispersive spectroscopy (EDS), XPS	EDS system (Oxford Instruments, UK) the chemical analysis of the sample He–Ne laser 532 nm as an excitation wavelength
5	Dielectric properties	Dielectric constant and dielectric loss	LCR meter
6	Magnetic properties	Retentivity and coercivity	Vibrational sample magnetometer
7	Electrochemical properties	Cyclic voltammetry, Chronopotentiometry and EIS	CHI608 instrument

This solution combustion method was executed due to availability of resources. The work of Byoung et al. highlights the importance of choosing a better method of synthesis in order to have a better electrochemical performance of synthesized material (Lee et al. 2016).

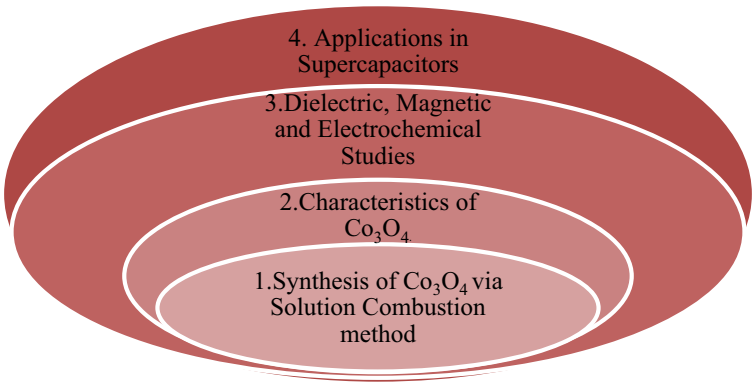

Representation of the study conducted in this paper.

Material characterization

The information on studies on structural properties and chemical analysis of as prepared nanospheres is given below.

Preparation of electrode

The working electrode is prepared using synthesized black Co_3O_4 nanopowder at 80%, to improve electrical conductivity carbon black taken at 10% and the excellent binder which combines both carbon black and Co_3O_4, namely polyvinylidene fluoride taken at 10%. The above mixture was grinded for an hour. Then, it was homogenized with excellent polar solvent named N-methyl-2-pyrrolidone. This was followed by adhering the slurry on an activated and chemically cleaned 3D nickel foam substrate. Finally, the solvent was evaporated from the prepared electrode by heating in hot air oven for 2 h at 100 °C.

Preparation of 3 electrode cell

To explore the essential electrochemical behavior of Co_3O_4 nanospheres, a three-electrode glass cell was set up. Details

Table 2 Three-electrode system setup

S. No.	Name of the electrode	Material used
1	Working electrode	Synthesized porous Co_3O_4 nanospheres
2	Reference electrode	Ag/AgCl
3	Counter electrode	Platinum foil
4	Electrolyte	KOH, NaOH, Na_2SO_4 and K_2SO_4
5	Substrate	3D Nickel foam

Table 3 Parameter in Debye–Scherrer formula

S. No.	Parameter	Physical quantity	Value/unit
1	D	Crystallite size	nm
2	k	Scherrer constant	0.94
3	λ	Wavelength of X-rays	0.15406 nm
4	β	Full width at half maximum	
5	θ	Bragg's angle	Degree

Table 4 Parameter in specific capacitance formula

S. No.	Parameter	Physical Quantity	unit
1	C	Specific capacitance	Fg^{-1}
2	$\int I\,(V)dv$	Algebraic sum of current	ampere
3	ΔV	Scan rate	Vs^{-1}
4	m	Mass of the active material in the electrode	gram
5	V_2–$V1$	Potential window	volt

of the three-electrode system are provided in Tables 2, 3 and 4.

Results and discussion

XRD analysis

The typical X-ray powder diffraction spectrum of as-synthesized porous Co_3O_4 nanospheres recorded in the diffraction angle 20°–80° is displayed in Fig. 1a. The XRD pattern revealed the (311) predominant orientation peak at $2\theta = 37.19°$ with other different characterization peaks (220), (222), (400), (422), (511), (440) at Bragg angles 31.48°, 38.3°, 44.57°, 56.24°, 60° and 65.66° respectively, indicating the presence of crystalline Co_3O_4 (Packiaraj et al. 2019). All reflection peaks are indexed to the cubic structure of Co_3O_4 with Fd $\bar{3}$ m (227) space group with lattice constant, $a = 8.072$ Å. The average crystalline size of the synthesized Co_3O_4 nanospheres is calculated using the following Debye–Scherrer Eq. (1) (Packiaraj et al. 2019) from the major diffraction peak (311) and is found to be 8 nm

$$D = \frac{k\lambda}{\beta \cos\theta} \tag{1}$$

Raman spectroscopy

As shown in Fig. 1b, Raman spectra of Co_3O_4 synthesized nanospheres were recorded in the range 350–750 cm^{-1} to determine the vibrational modes present in the sample. The Raman spectrum shows distinct peaks at 472, 510, 609 and 677 cm^{-1}, which proved the Co_3O_4 structure, support the XRD findings. The work of as-referred Diallo et al. highlights that the Co_3O_4 with Co^{2+} ($3d_7$) and Co^{3+} ($3d_6$) located at tetrahedral and octahedral sites, respectively, crystallizes in a spinel configuration and further added that all observed modes are in good agreement with the presence of pure cobalt oxide (Diallo et al. 2015). As shown in Fig. 1b, the main peak located at 677 cm^{-1} corresponding to Co^{3+} in octahedral coordination and Co–O vibrations due to stretching (double-degenerate E_g symmetrical mode). The peak at 472 cm^{-1} (E_g symmetry mode) is due to Co–O out-of-plane bending vibration and 510 cm^{-1} due to bridge oxygen (Co–O–Co) which has asymmetric stretching. All of the peaks in the spectrum are indicating typical Raman spectrum of cubic structured Co_3O_4 and its purity.

FTIR analysis

Chemical bonds in the sample prepared are shown by vibrational studies on Co_3O_4 prepared by FTIR with 500–4000 cm^{-1} being the range of wavenumber in Fig. 1c. The absorption broad band at 3735.45 cm^{-1} is attributed to O–H. The absorption bands around 1038.25 cm^{-1} and 1516.55 cm^{-1} may be attributed to O–H bending vibrations combined with Co atoms. The strong absorption band observed at 659.51 cm^{-1} is attributed to stretching vibration mode of Co^{+2}–O bonds which are tetrahedral sites. The second band at 551.39 cm^{-1} is due to stretching vibrational mode of Co^{+3}–O at octahedral sites. The FTIR characteristic peaks further proved the spinel structure of cobalt oxide. The above vibrational studies are elucidated by the important work on cobalt oxide characterization which concludes the spinel Co_3O_4 (Simonot et al. 1997; Toniolo et al. 2010).

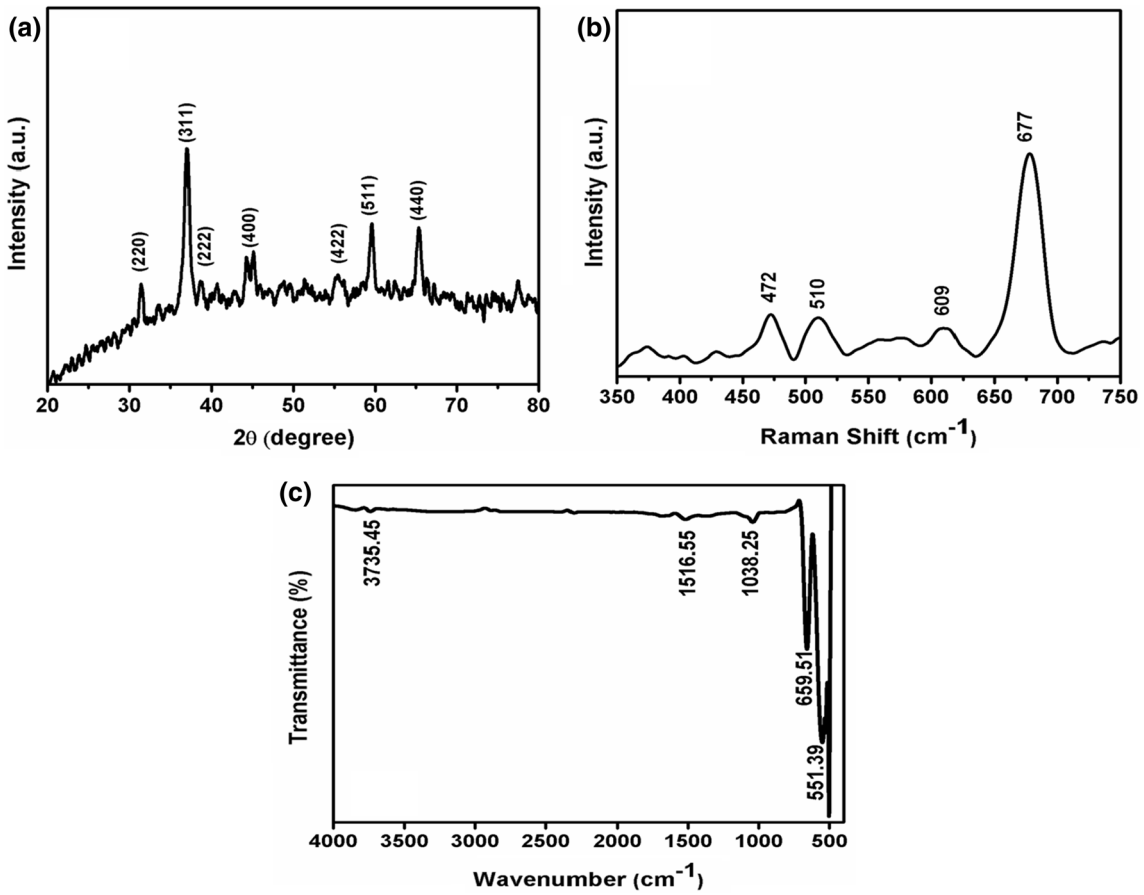

Fig. 1 **a** XRD, **b** Raman, **c** FTIR spectrum of porous Co_3O_4 nanospheres

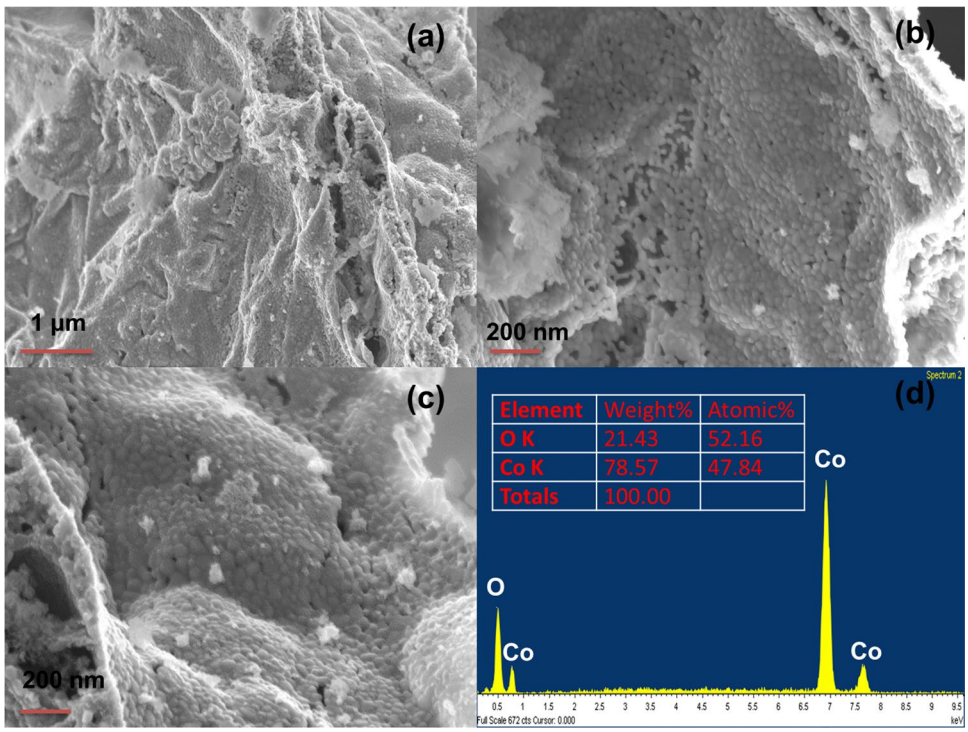

Fig. 2 **a**, **b** and **c** SEM micrographs in different magnifications, **d** EDS spectrum of Co_3O_4

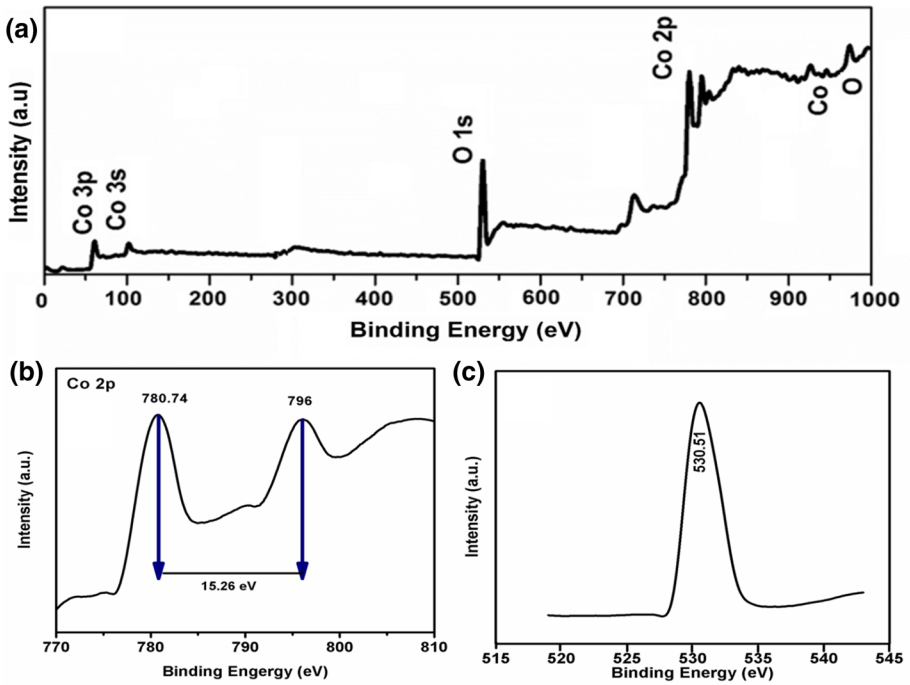

Fig. 3 XPS spectra of Co_3O_4 nanospheres **a** survey spectrum, **b** Co 2p spectrum, **c** O 1 s spectrum

SEM and EDS analysis

The SEM analysis has been executed to examine the morphology of porous Co_3O_4 nanospheres which are prepared. It is observed that the morphology consists of agglomerated spheres with small pores. 30 nm being the average size as depicted in Fig. 2a, b and c, which vividly shows the symmetrical nature of the spheres. This small-size and nanoporous morphology of the synthesized nanospheres enhances the electrochemical performance of supercapacitors and hence makes it good electrode material in supercapacitors. The above statement is supported by earlier research reports of SEM micrographs where presence of more active ions in porous electrode enhances specific capacitance by pseudocapacitance effect (Eslam et al. 2018) and also that $NiCo_2O_4$ nanoparticles with good spherical morphology possess superior specific capacitance which will be considered as good candidate for supercapacitor electrode applications (Priyadharshini and Ganesh. 2017).

EDS was performed to investigate the chemical composition of the newly formed porous Co_3O_4 nanospheres. The EDS spectrum shows presence of only elements cobalt and oxygen, indicating complete chemical reduction of the hexahydrated $Co(NO_3)_2{\cdot}6H_2O$ precursor (Diallo et al. 2015). EDS measurement is shown in Fig. 2d which shows corresponding binding energy peaks of Co and O present in the sample. Added to this, the synthesized samples purity is also reflected in EDS studies with 78.57% being the estimated

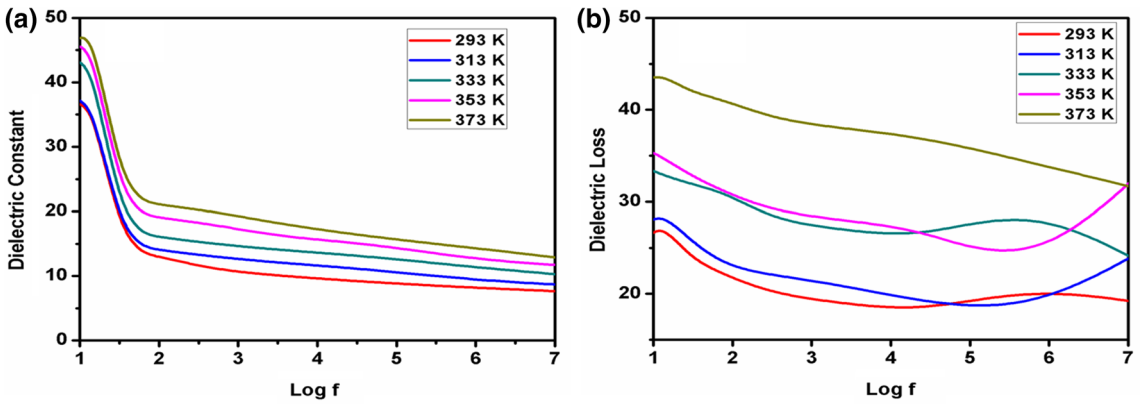

Fig. 4 **a** Dielectric constant vs frequency and **b** dielectric loss vs frequency

amount of Co and 21.53%.The presence of only cobalt and oxygen revealed by EDS also is an indication of complete combustion as reflected by the work of Toniolo et al. which is due to the characteristics of chemical reagents such as the fuels consumed and the oxidant nature of nitrate (Toniolo et al. 2010).

XPS studies

XPS is a surface-sensitive process which provides information about atomic composition and oxidation states of the samples. Figure 3a shows the XPS survey spectrum of Co_3O_4 nanospheres. Figure 3b shows the Co 2P spectrum of prepared sample where the two peaks clearly indicate two oxidation states. It displays Co $2p_{3/2}$ and Co $2p_{½}$ with peaks at binding energies observed at 780.74 and 796 eV phases or species intrinsic to the surface of spinel. This indicates the type of surface termination for the spinel orientation which shows presence of Co^{+2} and Co^{+3} cations. According to the findings (Yildirim and Kilis 2019), a spinel orientation contains two Co^{+2} cations in the tetrahedral sites, two Co^{+3} cations in the octahedral sites and four O^{-2} anions which is close to the present study including the separation of the peaks 15.26 eV. Figure 3c represents O1s spectra at 530.51 eV binding energy.

Dielectric properties

Dielectric constant

Figure 4a depicts the variation of Co_3O_4's dielectric constant with frequency. It is observed that the dielectric constant drops as the frequency rises. At lower frequencies, the value of dielectric constant is significantly higher. As frequency rises, it gets smaller and drops to extremely low at high frequencies where it is frequency independent. Similar types of behavior have also seen by other studies (Numan et al. 2016; DPMD Shaik et al. 2021). Space charge polarization may provide an explanation for the fluctuation in the dielectric constant. It is made up of several well-conducting grains that are spaced apart by thin, in conductive grain borders. The local movement of electrons in the direction of the electric field, which controls the polarization in Co_3O_4, is what causes the electronic exchange between Co^{2+} and Co^{3+}. With increasing frequency, polarization falls off until it reaches a constant value. This is due to the fact that the electron exchange Co^{2+} and Co^{3+} cannot follow the alternating field above a specific amount of external field frequency (Zhang et al. 2017; Salunkhe et al. 2015).

Dielectric loss

Figure 4b depicts the variation of dielectric loss with frequency. It is observed that with an increase in frequency, dielectric loss decreases. The reason for this is because as frequency rises, polarization decreases. It eventually settles on a fixed value (Liu et al. 2016). At lower frequencies, dielectric loss has a significant value. The prevalence of species including Co^{2+} ions, oxygen vacancies, grain boundary defects, interfacial dislocation pileups, voids, etc., is the reason (Salunkhe et al. 2015; Wen et al. 2012). Due to any species contributing to polarizability being discovered to lag behind the applied electric field at higher frequencies, the decreasing trend in with an increase in frequency is natural (Zhang et al. 2013).

Magnetic properties

The magnetic properties of Co_3O_4 nanospheres at 5 and 300 K temperatures are shown in Fig. 5. As shown in Fig. 5, the hysteresis curve of Co_3O_4 nanospheres prepared at 473 K displays a ferromagnetic behavior at both the temperatures (5 and 300 K) with a saturation magnetization of 0.113 emu g^{-1} at the maximum field of 8.9 kOe applied. The ferromagnetic behavior of the sample could be attributed to the uncompensated surface spins and finite size effects (Reddy et al. 2021; Sylla et al. 2019; Yang et al. 2007).

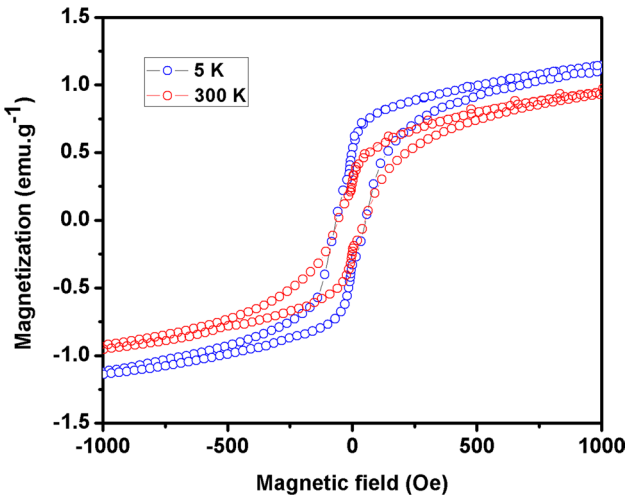

Fig. 5 Magnetization vs magnetic field of Co_3O_4 nanospheres

Electrochemical properties

The electrochemical properties of synthesized Co_3O_4 nanospheres with porous framework and increased surface area are evaluated by cyclic voltammetry (CV), chronopotentiometry (CP) and electrochemical impedance spectroscopy (EIS) using a three-electrode aqueous method. Here, Co_3O_4 is used as a working electrode, Ag/AgCl as a counter, and platinum foil as a reference electrode and four electrolytic

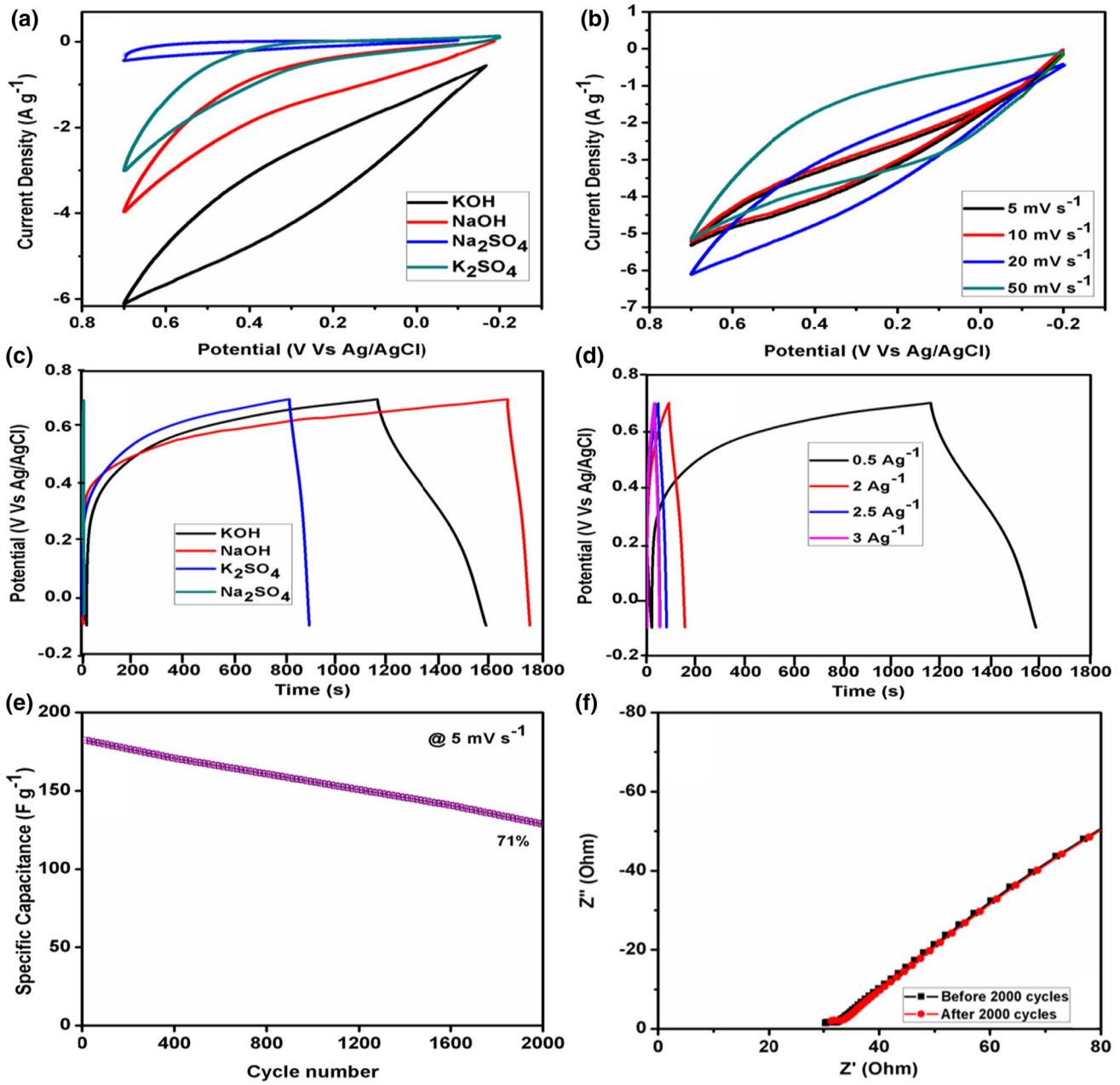

Fig. 6 **a** CV curves of porous Co_3O_4 nanospheres in different electrolytes at 5 mVs^{-1}, **b** CV curves of the sample in 1 M KOH at different scan rates, **c** charge–discharge curves in different electrolytes, **d** charge–discharge curves at different current densities in 1 M KOH, **e** specific capacitance with cycle number, **f** Nyquist plot before and after 2000 cycles

Table 5 The relationship of hydrated ionic size and conductivity for the electrolytes utilized

Hydrated ion	Potassium ion hydrated	Sodium ion hydrated	Hydroxide ion hydrated	Sulfate ion hydrated
Hydrated ion size	3.31 Å	3.58 Å	3.0 Å	3.79 Å
Conductivity (Inversely proportional to the size)	Higher than sodium		Higher than sulfate	

Table 6 Parameter in discharge specific capacitance formula

S. No.	Parameter	Physical quantity	unit
1	C	Specific capacitance	Fg^{-1}
2	$\int I\,(V)dv$	Current	ampere
3	Δt	Discharge time	Vs^{-1}
4	m	Mass of the active material in the electrode	gram
5	ΔV	Potential window	volt

solutions of KOH, NaOH, Na_2SO_4 and K_2SO_4 are used. Figure 6a shows the cyclic voltammetry (CV) curves of the porous Co_3O_4 nanospheres at scan rate 5 mVs^{-1} having −0.2–+0.8 V as potential window in the above aqueous electrolytes. The CV curves display the capacitive-like characteristics from the quick reversal in the currents during the change in the potential direction (Naresh et al. 2019). In addition, CV curves show quasi-rectangular shape and more area in 1 M KOH electrolyte when compared to aqueous solutions of NaOH, Na_2SO_4 and K_2SO_4 which shows better electrochemical performance. The values of specific capacitance of the prepared sample were calculated using Eq. (2):

$$C = \frac{\int I\,(V)dv}{2m(V2 - V1)\Delta V} \tag{2}$$

The specific capacitance values are 175 Fg^{-1} (KOH), 97 Fg^{-1} (NaOH), 64 Fg^{-1} (K_2SO_4) and 29 Fg^{-1} (Na_2SO_4) at 5 mVs^{-1} scan rate in various electrolyte solutions. The better electrochemical performance of porous Co_3O_4 nanospheres in aqueous KOH solution, when compared to other electrolytes like NaOH, Na_2SO_4 and K_2SO_4, is due to the greater size of hydrated Na^+ ion than that of hydrated K^+ ion. Added to this, other parameter is ionic conductivity which depends on ionic size that will be lower for Na^+ ion hydrated compared to K^+ ion. The hydrated ion size and their conductivities are compiled in Table 5.

Therefore, SO_4^- has lower ionic conductivity than OH^- due to larger size. The ionic conductivity variation in water and other solvents exhibits an anomalous dependence on the ionic radius. Molecular dynamics simulations suggest that this has origin in the levitation effect which suggests that the diffusivity is maximum for the ion with diameter comparable to the neck diameter of the void network within the solvent. The origin of such an anomalous dependence lies in the mutual cancellation of forces (Rahimi-Nasrabadi et al. 2017; Kumar and Yashonath 2019). The CV curves of Co_3O_4 in 1 M KOH at different scan rates are shown in Fig. 6b. The specific capacitance values are calculated using Eq. (2) and are found to be 175, 148, 104 and 77 Fg^{-1} at 5, 10, 20 and 50 mVs^{-1}, respectively. The study shows that at lower scan rates, K^+ electrolytic cations penetrate into the pores of the material which leads to higher capacitance, whereas at greater scan rates they are on outer surface of the material which results in lower capacitance.

The galvanostatic charge–discharge measurements of the Co_3O_4 nanospheres in four electrolytes are carried out at 0.5 $Ag.^{-1}$ current density. The almost symmetric nature of the charge–discharge curves of Co_3O_4 in KOH electrolyte shows good electrochemical reversibility of the electrode. At the same time, Co_3O_4 shows greater discharge time in KOH electrolyte (Fig. 6c) which leads to greater discharge capacitance. The discharge specific capacitance values are calculated using Eq. (3) (Table 6)

$$C = \frac{I\Delta t}{m\Delta V} \tag{3}$$

The Co_3O_4 nanospheres discharge specific capacitance in various electrolyte solutions are 182 Fg^{-1} (KOH), 106 Fg^{-1} (NaOH), 73 Fg^{-1} (K_2SO_4) and 37 Fg^{-1} (Na_2SO_4). It is to be noted that the higher specific capacitance of 182 Fg^{-1} was exhibited by Co_3O_4 which is in support with CV results. Figure 6d represents the Co_3O_4 charge–discharge curves at 0.5 Ag^{-1} current density in 1 M KOH electrolyte solution. The galvanostatic charge–discharge measurements of the Co_3O_4 nanospheres in 1 M KOH are carried out at different current densities ranging from 0.5 to 3 Ag^{-1} and are presented in Fig. 6d. The symmetric nature of the charge–discharge curves of Co_3O_4 in KOH electrolyte shows good electrochemical reversibility of the electrode. The specific capacitance value is calculated using Eq. (3) and is found to be 182, 154, 118 and 81 Fg^{-1} at 0.5, 2, 2.5 and 3 Ag^{-1}, respectively.

Added to specific capacitance values, long-term cyclic stability is a good electrochemical characterization study to assess the fabricated porous Co_3O_4 nanospheres as electrode in 1 M KOH electrolyte. Figure 6e shows that after 2000 continuous cycles at 5 mVs^{-1} scan rate the prepared sample had 71% capacitive retention than initial value (Yang et al. 2007; Kumar and Yashonath 2019). There is a decrease in specific capacitance value with cycle number as active material is used up in the electrolyte during the early charging/discharging cycles (Wang et al. 2013) as shown in Fig. 6e. The high SCs achieved for Co_3O_4 nanospheres may be owing to the improved electric double-layer capacitance behavior of the sample. In particular, this porous nanostructure of Co_3O_4 can act as an "ion buffer reservoir" (Wang et al. 2013; Priyadharsini et al. 2020; Huang et al. 2019; Dezfuli et al. 2015). These findings have shown that with better cyclic stability of porous Co_3O_4 electrode it may be a long-lasting candidate for electrode material for next-generation electrochemical energy storage applications.

Table 7 Comparison between capacitive performance of fabricated electrode and those reported for Co_3O_4 in the literature

S. No.	Material	Method of preparation	Electrolyte	Specific capacitance	Scan rate/ Current density	Retention	Cycles	References
1	Co_3O_4 ultrafine nanocrystals	Laser ablation in liquid	Polyvinyl alcohol/phosphoric acid	177 Fg^{-1}	1 mv s^{-1}	100%	20,000	Liu et al. (2016)
2	Co_3O_4 Nanoparticles in mesoporous carbon	Pyrolysis followed by low-temperature oxidation	2 M KOH	54 Fg^{-1}	0.1 A g^{-1}	82%	10,000	Zallouz et al. (2021)
3	Co_3O_4 Nanoparticles	sol–gel	3 M KOH	761.25 Fg^{-1}	11 ma/Cm^2	100%	500	Kumar and Yashonath (2019)
4	Co_3O_4 Nanoparticles	Accelerated thermochemical conversion	6 M KOH	162 Fg^{-1}	2.75ag^{-1}	72.2%	1000	Tummala et al. (2012)
5	Co_3O_4 Nanoparticles	Chemical reflux method	2 M KOH	1413 Fg^{-1}	1 Ag^{-1}	98.4%	1000	Packiaraj et al. (2019)
6	Co_3O_4 Nanoparticles	Solvothermal	2 M KOH	476 Fg^{-1}	0.5 Ag^{-1}	82%	2000	Deori et al. (2013)
7	Co_3O_4 Nanospheres	Solution combustion	1 M KOH	182 Fg^{-1}	0.5 Ag^{-1}	71%	2000	This work

The electrochemical impedance spectroscopy is a core technique for studying the kinetic behavior of the ions in an electrolyte, and Fig. 6f represents EIS analysis of synthesized Co_3O_4 in 1 M KOH aqueous solution over a frequency range of 1 Hz–1 MHz. In Nyquist plots, at high-frequency region, the solution resistance (R_s) is taken by the intersection made on horizontal axis. Increase in solution resistance from 4–5Ω after 2000 cycles was the key observation. Charge transfer resistance (R_{ct}) is the semicircle in high to medium-frequency region in the Nyquist plot. It was observed that after 2000 cycles the R_{ct} of the porous sample was increased to 8–6Ω. The increase in R_s and R_{ct} values after 2000 cycles suggests the decrease in specific capacitance with increase in cycle number. The characteristic behavior of supercapacitor is reflected in the synthesized sample by diffusive resistance in low-frequency region with a straight line behavior. Table 7 shows the comparison of the present work with previous literature.

Conclusion

Porous Co_3O_4 nanospheres are successfully prepared by a solution combustion technique at low temperatures for supercapacitor applications. XRD and Raman data were confirmed cubic structure of Co_3O_4 with an estimated crystallite size of 8 nm. SEM studies revealed a spherical shape of grains with an average grain size of 30 nm. The dielectric studies proved the frequency dependence of dielectric constant and dielectric loss. The magnetic properties of porous Co_3O_4 showed ferromagnetic nature of the sample. The electrochemical studies of Co_3O_4 nanospheres exhibited a specific capacitance of 182 Fg^{-1} at 0.5 Ag^{-1} current density in 1 M KOH aqueous electrolyte. The porous Co_3O_4 nanosphere electrode with good capacitive retention during cycling makes it a future potential candidate for supercapacitors. To further enhance the capacitive performance of Co_3O_4, the study can be extended at various fuel-to-oxidation ratios and optimizing the synthesis and annealed temperature.

Acknowledgements The authors acknowledge Dr. Anoop Mukharjee, Assistant Professor, and Mrs. Babita Mukharjee, Lecturer, from Prince Sultan University, Riyadh, Saudi Arabia, for their support in checking the plagiarism time to time.

References

Deori K, Ujjain SK, Sharma RK, Deka S (2013) Morphology controlled synthesis of nanoporous Co_3O_4 nanostructures and their charge storage characteristics in supercapacitors. ACS Appl Mater Interface 5(21):10665–10672. https://doi.org/10.1021/am4027482

Dezfuli AS, Ganjali MR, Naderi HR, Norouzi P (2015) A high performance supercapacitor based on a ceria/graphene nanocomposite synthesized by a facile sonochemical method. RSC Adv 5(57):46050–46058. https://doi.org/10.1039/c5ra02957k

Diallo A, Beye AC, Doyle TB, Park E, Maaza M (2015) Green synthesis of Co_3O_4 nanoparticles via aspalathus linearis: physical properties. Green Chem Lett Rev 8(3–4):30–36. https://doi.org/10.1080/17518253.2015.1082646

Eslam KFC, Aboelazm AA, Gomaa-Ali AM (2018) Cobalt oxide supercapacitor electrode recovered from spent lithium-ion battery. Chem Adv Mater 3(4):67–74

Farhadi S, Pourzare K, Sadeghinejad S (2013) Simple preparation of ferromagnetic Co_3O_4 nanoparticles by thermal dissociation of the

[CoII(NH_3)$_6$](NO_3)$_2$ complex at low temperature. J Nanostruct Chem 3(1):4–10. https://doi.org/10.1186/2193-8865-3-16
Gu F, Li C, Hu Y, Zhang L (2007) Synthesis and optical characterization of Co_3O_4 nanocrystals. J Cryst Growth 304(2):369–373. https://doi.org/10.1016/j.jcrysgro.2007.03.040
Hall PJ et al (2010) Energy storage in electrochemical capacitors: designing functional materials to improve performance. Energy Environ Sci 3(9):1238–1251. https://doi.org/10.1039/c0ee00004c
Huang D, Liu H, Li T, Niu Q (2019) Template-free synthesis of NiO skeleton crystal octahedron and effect of surface depression on electrochemical performance. J Sol-Gel Sci Technol 89(2):511–520. https://doi.org/10.1007/s10971-018-4908-3
Kumar P, Yashonath S (2019) Ionic conductivity in aqueous electrolyte solutions: insights from computer simulations. J Mol Liq 277:506–515. https://doi.org/10.1016/j.molliq.2018.12.090
Lee BS et al (2016) Silicon/carbon nanotube/$BaTiO_3$ nanocomposite anode: evidence for enhanced lithium-ion mobility induced by the local piezoelectric potential. ACS Nano 10(2):2617–2627. https://doi.org/10.1021/acsnano.5b07674
Liu XY, Gao YQ, Yang GW (2016) A flexible, transparent and super-long-life supercapacitor based on ultrafine Co_3O_4 nanocrystal electrodes. Nanoscale 8(7):4227–4235. https://doi.org/10.1039/c5nr09145d
Mirzaeian M et al (2017) Electrode and electrolyte materials for electrochemical capacitors. Int J Hydrogen Energy 42(40):25565–25587. https://doi.org/10.1016/j.ijhydene.2017.04.241
Naresh-Kumar-Reddy P, Shaik DP, Ganesh V, Nagamalleswari D, Thyagarajan K, Vishnu Prasanth P (2019) Structural, optical and electrochemical properties of TiO_2 nanoparticles synthesized using medicinal plant leaf extract. Ceram Int 45(13):16251–16260. https://doi.org/10.1016/j.ceramint.2019.05.147
Naresh Kumar Reddy P, Shaik DPMD, Ganesh V, Nagamalleswari D, Thyagarajan K, Vishnu Prasanth P (2021) High electrochemical activity of 3D flower like nanostructured TiO_2 obtained by green synthesis. Appl Surf Sci 561(May):150092. https://doi.org/10.1016/j.apsusc.2021.150092
Numan A, Duraisamy N, Saiha Omar F, Mahipal YK, Ramesh K, Ramesh S (2016) Enhanced electrochemical performance of cobalt oxide nanocube intercalated reduced graphene oxide for supercapacitor application. RSC Adv 6(41):34894–34902. https://doi.org/10.1039/c6ra00160b
Packiaraj R, Devendran P, Venkatesh KS, Asath-Bahadur S, Manikandan A, Nallamuthu N (2019) Electrochemical investigations of magnetic Co_3O_4 nanoparticles as an active electrode for supercapacitor applications. J Supercond Nov Magn 32(8):2427–2436. https://doi.org/10.1007/s10948-018-4963-6
Priyadharshini BST, Ganesh GRV (2017) Hydrothermal synthesis of spherical $NiCO_2O_4$ nanoparticles as a positive electrode for pseudocapacitor applications. J Sol-Gel Sci Technol. https://doi.org/10.1007/s10971-017-4504-y
Priyadharsini CI et al (2020) Sol–Gel synthesis of Co_3O_4 nanoparticles as an electrode material for supercapacitor applications. J Sol-Gel Sci Technol 96(2):416–422. https://doi.org/10.1007/s10971-020-05393-x
Rahimi-Nasrabadi M, Naderi HR, Karimi MS, Ahmadi F, Pourmortazavi SM (2017) Cobalt carbonate and cobalt oxide nanoparticles synthesis, characterization and supercapacitive evaluation. J Mater Sci Mater Electron 28(2):1877–1888. https://doi.org/10.1007/s10854-016-5739-z
Reddy PNK, Shaik DPMD, Nagamalleswari D, Thyagarajan K, Prasanth PV (2021) Electrochemical activity of TiO_2 nanoparticles in NaOH electrolyte via green synthesis using calotropis gigantea plant leaf extract. Indian J Sci Technol 14(34):2766–2772. https://doi.org/10.17485/ijst/v14i34.1424
Salunkhe RR, Tang J, Kamachi Y, Nakato T, Kim JH, Yamauchi Y (2015) Asymmetric supercapacitors using 3D nanoporous carbon and cobalt oxide electrodes synthesized from a single metal-organic framework. ACS Nano 9(6):6288–6296. https://doi.org/10.1021/acsnano.5b01790
Shaik DPMD, Rosaiah P, Ganesh KS, Qiu Y, Hussain OM (2018) Improved electrochemical performance of Mn_3O_4 thin film electrodes for supercapacitors. Mater Sci Semicond Process 84:83–90. https://doi.org/10.1016/j.mssp.2018.03.013
Shaik DPMD, Kumar MVS, Reddy PNK, Hussain OM (2021) High electrochemical performance of spinel Mn_3O_4 over Co_3O_4 nanocrystals. J Mol Struct 1241:130619. https://doi.org/10.1016/j.molstruc.2021.130619
Simonot L, Garin F, Maire G (1997) A comparative study of $LaCoO_3$, Co_3O_4 and $LaCoO_3$–Co_3O_4: I. Preparation, characterisation and catalytic properties for the oxidation of CO. Appl Catal B Environ 11(2):167–179. https://doi.org/10.1016/S0926-3373(96)00046-X
Sylla NF et al (2019) Effect of porosity enhancing agents on the electrochemical performance of high-energy ultracapacitor electrodes derived from peanut shell waste. Sci Rep 9(1):1–15. https://doi.org/10.1038/s41598-019-50189-x
Toniolo JC, Takimi AS, Bergmann CP (2010) Nanostructured cobalt oxides (Co_3O_4 and CoO) and metallic Co powders synthesized by the solution combustion method. Mater Res Bull 45(6):672–676. https://doi.org/10.1016/j.materresbull.2010.03.001
Tummala R, Guduru RK, Mohanty PS (2012) Nanostructured Co_3O_4 electrodes for supercapacitor applications from plasma spray technique. J Power Source 209:44–51. https://doi.org/10.1016/j.jpowsour.2012.02.071
Wang J, Du N, Wu H, Zhang H, Yu J, Yang D (2013) Order-aligned Mn_3O_4 nanostructures as super high-rate electrodes for rechargeable lithium-ion batteries. J Power Source 222:32–37. https://doi.org/10.1016/j.jpowsour.2012.08.056
Wang X, Yan C, Sumboja A, Lee PS (2014) High performance porous nickel cobalt oxide nanowires for asymmetric supercapacitor. Nano Energy 3:119–126. https://doi.org/10.1016/j.nanoen.2013.11.001
Wen W, Wu JM, Tu JP (2012) A novel solution combustion synthesis of cobalt oxide nanoparticles as negative-electrode materials for lithium ion batteries. J Alloy Compd 513:592–596. https://doi.org/10.1016/j.jallcom.2011.11.019
Yang CM et al (2007) Nanowindow-regulated specific capacitance of supercapacitor electrodes of single-wall carbon nanohorns. J Am Chem Soc 129(1):20–21. https://doi.org/10.1021/ja065501k
Yildirim Z, Kilis S (2019) Posting patterns of students' social presence, cognitive presence, and teaching presence in online learning. Online Learn J. https://doi.org/10.24059/olj.v23i2.1460
Zallouz S, Réty B, Vidal L, Le-Meins JM, Matei-Ghimbeu C (2021) Co_3O_4 Nanoparticles embedded in mesoporous carbon for supercapacitor applications. ACS Appl Nano Mater 4(5):5022–5037. https://doi.org/10.1021/acsanm.1c00522
Zhang X, Yu P, Zhang D, Zhang H, Sun X, Ma Y (2013) Room temperature synthesis of Mn_3O_4 nanoparticles: characterization, electrochemical properties and hydrothermal transformation to γ-MnO_2 nanorods. Mater Lett 92:401–404. https://doi.org/10.1016/j.matlet.2012.11.022
Zhang H, Nai J, Yu L, David-Lou XW (2017) Metal-organic-framework-based materials as platforms for renewable energy and environmental applications. Joule 1(1):77–107. https://doi.org/10.1016/j.joule.2017.08.008